

Distinct electronic nematicities between electron and hole underdoped iron pnictides

J. J. Ying¹, X. F. Wang¹, T. Wu¹, Z. J. Xiang¹, R. H. Liu¹, Y. J. Yan¹, A.

F. Wang¹, M. Zhang¹, G. J. Ye¹, P. Cheng¹, J. P. Hu² and X. H. Chen^{1*}

¹Hefei National Laboratory for Physical Science at Microscale and Department of Physics,
University of Science and Technology of China, Hefei, Anhui 230026, People's Republic of China

²Department of Physics, Purdue University, West Lafayette, Indiana 47907, USA

We systematically investigated the in-plane resistivity anisotropy of electron-underdoped $EuFe_{2-x}Co_xAs_2$ and $BaFe_{2-x}Co_xAs_2$, and hole-underdoped $Ba_{1-x}K_xFe_2As_2$. Large in-plane resistivity anisotropy was found in the former samples, while *tiny* in-plane resistivity anisotropy was detected in the latter ones. When it is detected, the anisotropy starts above the structural transition temperature and increases smoothly through it. As the temperature is lowered further, the anisotropy takes a dramatic enhancement through the magnetic transition temperature. We found that the anisotropy is universally tied to the presence of non-Fermi liquid T-linear behavior of resistivity. Our results demonstrate that the nematic state is caused by electronic degrees of freedom, and the microscopic orbital involvement in magnetically ordered state must be fundamentally different between the hole and electron doped materials.

PACS numbers: 74.25.-q, 74.25.F-, 74.70.Xa

The newly discovered iron-based high temperature superconductors provide a new family of materials to explore the mechanism of high- T_c superconductivity besides high- T_c cuprates superconductors[1–4]. The parent compounds undergo a tetragonal to orthorhombic structure transition and a collinear antiferromagnetic (CAFM) transition. The structure transition temperature(T_S) is higher than the CAFM transition temperature(T_N) in 1111 system, while for the 122 parent compound T_N is almost the same with T_S . Superconductivity arises when both transitions are suppressed via electron or hole doping. The origin of the structure transition and CAFM transition is still unclear, it was proposed that antiferromagnetic fluctuation [6, 7] or orbital ordering[5, 17, 18] may play an important role in driving the transitions.

Recent works showed a large in-plane resistivity anisotropy below T_S or T_N in Co-doped Ba122 system, though the distortion of the orthorhombic structure is less than 1 % [8, 9] in the CAFM state. The resistivity is smaller along the antiferromagnetic a direction than along the ferromagnetic b direction which is opposite to our intuitive thinking. Moreover, the resistivity anisotropy grows with doping and approaches its maximum close to the point where superconductivity emerges. Other experiments also reported the existence of anisotropy in many different physical properties in the CAFM state of iron pnictides including magnetic exchange coupling[14], Fermi surface topology[15] and local density distribution[16]. Electronic anisotropies have also been observed in many other materials, including underdoped cuprates, quantum Hall systems and

$Sr_3Ru_2O_7$ [12, 13]. In cuprates, electronic anisotropy can not be explained by small structural orthorhombicity[10, 11] and it has been proposed the large electron anisotropy is due to the emergence of electron nematic phase. This idea has been widely investigated in the other two systems as well. In iron-pnictides, the origin of the electronic anisotropy is still elusive because of their complicated electronic structures and the presence of many different degrees of freedom.

In this paper, we systematically investigated the in-plane resistivity anisotropy of electron-underdoped $EuFe_{2-x}Co_xAs_2$ and $BaFe_{2-x}Co_xAs_2$, and hole-underdoped $Ba_{1-x}K_xFe_2As_2$ systems. Large in-plane resistivity behavior was found below T_S or T_N in $EuFe_{2-x}Co_xAs_2$ and $BaFe_{2-x}Co_xAs_2$, while in-plane anisotropy is dramatically decreased and barely observable in $Ba_{1-x}K_xFe_2As_2$. The resistivity shows T-linear behavior above the temperature wherever the resistivity anisotropy starts to emerge. In the $Ba_{1-x}K_xFe_2As_2$, no T-linear behavior in the resistivity is observed in the normal state. For $EuFe_{2-x}Co_xAs_2$, the resistivity behaves very differently at T_S and T_N . The in-plane anisotropy starts to emerge even above T_S and increases smoothly through it. As the temperature is lowered further, it takes a dramatic enhancement through the magnetic phase transition. Therefore, our results provide direct evidence ruling out the possibility that the anisotropy is caused by lattice distortion. The dramatic difference of the anisotropies in the electron and hole doped materials suggests that magnetism must be orbital-selective in a way that the magnetism in the hole underdoped iron-pnictides may stem mainly from the d_{xy} orbitals while the magnetism in the electron underdoped ones attributes mainly to the d_{yz} and d_{xz} orbitals.

High quality single crystals with nominal composition $EuFe_{2-x}Co_xAs_2$ ($x=0, 0.067, 0.1, 0.225$) and

*Corresponding author; Electronic address: chenxh@ustc.edu.cn

$Ba_{1-x}K_xFe_2As_2$ ($x=0.1, 0.18$) were grown by self-flux method as described elsewhere[19]. Many shining plate-like single crystals can be obtained. $EuFe_2As_2$ has not only a CAFM or structural transition around 190 K, but also an antiferromagnetic transition of Eu^{2+} ions around 20 K[20]. As Co-doping increases, the SDW transition and structure transition were gradually separated and suppressed like the $BaFe_{2-x}Co_xAs_2$ system. Resistivity reentrance behavior due to the antiferromagnetic ordering of Eu^{2+} spins is also observed at low temperature. The detailed in-plane resistivity of $EuFe_{2-x}Co_xAs_2$ can be found elsewhere[21, 22]. $Ba_{0.9}K_{0.1}Fe_2As_2$ and $Ba_{0.82}K_{0.18}Fe_2As_2$ undergoes structural transition and SDW transition at around 128K and 113 K, respectively. It is difficult to directly measure the in-plane resistivity anisotropy because the material naturally forms structure domains below T_S . In order to investigate the intrinsic in-plane resistivity anisotropy we developed a mechanical cantilever device that is able to detwin crystals similar to the Ref.8. Crystals were cut parallel to the orthorhombic a and b axes so that the orthorhombic $a(b)$ direction is perpendicular (parallel) to the applied pressure direction. ρ_a (current parallel to a) and ρ_b (current parallel to b) were measured on the same sample using standard 4-point configuration. We can get the same result with Ref.8 in Co-doped Ba122 system as shown in Fig.4(d) and (e).

Fig.1(a) shows the temperature dependence of in-plane resistivity with the current flowing parallel to the orthorhombic b direction (black) and orthorhombic a direction (red) of the detwinned $EuFe_2As_2$ sample. Compounds with a small amount of Co-doping show large in-plane anisotropy as displayed in Fig.1(b) and (c) for $x=0.067$ and $x=0.1$, respectively. More specifically, we can find a much more obvious upturn of ρ_b around T_N or T_S compared to the twinned in-plane resistivity as the blue line shows while ρ_a shows no upturn and drops very rapidly with the temperature decreases below T_N or T_S . The behavior of ρ_a is very similar to the $EuFe_2As_2$ polycrystalline samples[23]. When the Co-doping increases, the upturn of ρ_b at T_N or T_S becomes much more sharper while the drop of ρ_a at T_N or T_S gradually disappears and turns into a small upturn at the temperature slightly lower than ρ_b . For the sample of $x=0.225$, no in-plane anisotropy was found due to the complete suppression of the structural or magnetic transition as shown in Fig.1(d). The different behavior of ρ_a and ρ_b observed here is very similar to the ones in other parent or electron underdoped iron-pnictides[8, 9].

Further examining our data, we also notice that the structural transition temperature T_S and the magnetic transition temperature T_N become well separated as the Co-doping increases in $EuFe_{2-x}Co_xAs_2$. This separation provides us an opportunity to investigate the effects of the structural transition and magnetic transition on the ρ_a and ρ_b separately. The two transition tempera-

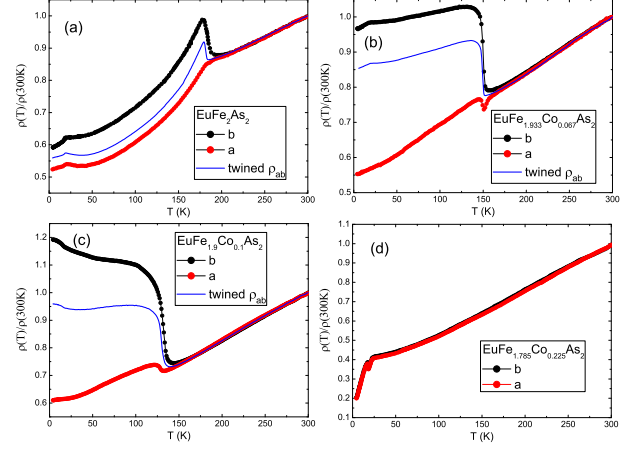


FIG. 1: (Color online) Temperature dependence of in-plane resistivity with the electric current flow along a direction (red) and b direction (black) respectively for the parent compound (a): $EuFe_2As_2$, (b): $EuFe_{1.933}Co_{0.067}As_2$, (c): $EuFe_{1.9}Co_{0.1}As_2$, (d): $EuFe_{1.775}Co_{0.225}As_2$. The twinned in-plane resistivity was also shown for comparison (blue line).

tures can be obtained by analyzing the heat capacity of the samples. Treating the heat capacity in the $x=0.225$ sample as phonon background and subtracting it, we obtain the electronic part of the heat capacity of the $x=0.067$ and $x=0.1$ samples, ΔC_P . Taking the $x=0.067$ sample as an example, the ΔC_P has two distinct features as a function of temperature: a very sharp peak at 150 K and a broad hump around 157 K. Similar to other isostructure materials, such as $BaFe_{2-x}Co_xAs_2$ [25], we can attribute the sharp peak to the magnetic transition and the broad hump to the structure transition. In the $x=0.067$ sample, as shown in fig.2(a), ρ_a shows a dip like behavior from T_S to T_N . ρ_a starts to drop rapidly at the temperature coincident with T_S , and after reaching its minimum value, it shows a very weak upturn at the temperature coincident with T_N . ρ_b , however, has no observable feature at T_S but shows a large upturn around T_N . When the sample is not detwinned, the in-plane resistivity ρ_{ab} also shows a large upturn. For the $x=0.1$ sample, T_S is suppressed to 140 K and T_N is suppressed to 130 K from the heat capacity measurement as shown in Fig.2(b). ρ_b starts to go upward above T_S but ρ_a does not show any obvious response. The $d\rho_{ab}/dT$ curve of the twinned ρ_{ab} peaks around T_N while the peak of $d\rho_b/dT$ is higher than T_N and the one of $d\rho_a/dT$ is slightly lower than T_N . With increasing the Co doping, the effect of the structure transition on the ρ_a is gradually wiped out which is similar to $BaFe_{2-x}Co_xAs_2$ system, while the upturn behavior T_N becomes more noticeable.

We characterized the degree of in-plane resistivity anisotropy by the ratio ρ_b/ρ_a . Fig.3(a) and (b) show in-

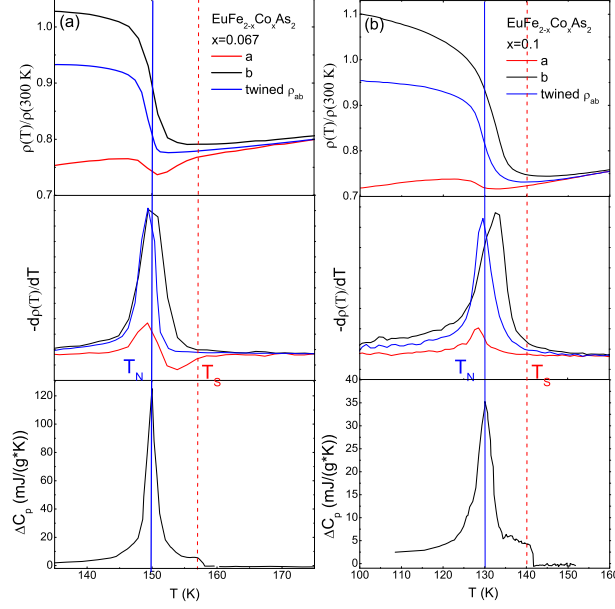


FIG. 2: (Color online) Temperature dependence of ρ_a , ρ_b and twined ρ_{ab} , their differential curve and heat capacity around the T_S and T_N for the sample of (a): $x=0.067$ and (b): $x=0.1$. The red dashed line and blue solid line indicated T_S and T_N respectively.

plane resistivity anisotropy ρ_b/ρ_a and its related differential curve for $x=0.067$ and $x=0.1$ samples, respectively. The amplitude of the anisotropy is greatly increased with Co doping though the magnetic transition and structure transition are suppressed, similar to $BaFe_{2-x}Co_xAs_2$. The in-plane resistivity anisotropy increases very rapidly at T_N and still gradually increases down to 4 K. A very sharp peak can be observed in the differential curve of ρ_b/ρ_a at the temperature coincident with T_N . However, ρ_b/ρ_a did not show any obvious anomaly at T_S . The sharp increase of in-plane resistivity anisotropy at T_N indicates that in-plane anisotropy is correlated to the magnetic transition rather than structure transition. It also indicates that the in-plane electron anisotropy is driven by the magnetic fluctuation or other hidden electronic order rather than the small orthorhombic distortion.

To understand the common feature of the in-plane resistivity anisotropies in $EuFe_{2-x}Co_xAs_2$ and $BaFe_{2-x}Co_xAs_2$, we plot ρ_a and ρ_b in an enlarged temperature region as shown in Fig.4(a), (b), (c), (d) and (e). For $EuFe_{2-x}Co_xAs_2$, it is very clear that the in-plane resistivity anisotropy emerges at temperatures higher than the structure transition temperature as the black arrows indicate. It suggests that fluctuations associated with the resistivity anisotropy must emerge well above the T_S . Moreover, T-linear resistivity behaviors appear in a large temperature region above the temperature which

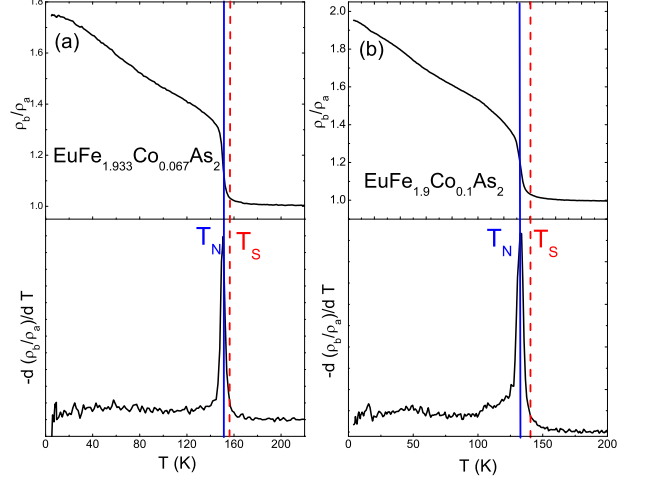


FIG. 3: (Color online) In-plane resistivity anisotropy ρ_b/ρ_a and its related differential curve for the sample of (a): $x=0.067$ and (b): $x=0.1$. The blue solid line indicated T_N and red dashed line indicated T_S .

ρ_a and ρ_b begin to show discrepancy. We also observed this kind of feature in Co-doped Ba122 system as shown in Fig.4(d), (e) for $BaFe_2As_2$ and $BaFe_{1.83}Co_{0.17}As_2$ respectively. This non-Fermi liquid behavior, or the T-linear behavior has also been observed in other iron pnictides, for example, $BaFe_2As_{2-x}P_x$ single crystals and $SmO_{1-x}F_xFeAs$ polycrystalline samples[26, 27]. It suggests that this behavior might be universal in electron underdoped iron pnictides at high temperature. The T-linear resistivity behavior is also similar to the one in cuprates. However, in $Ba_{2-x}K_xFe_2As_2$, such a T-linear behavior is rapidly suppressed through K doping. As shown in Fig.4(f) and (g), $Ba_{0.9}K_{0.1}Fe_2As_2$ shows very tiny in-plane anisotropy compared with its parent compound, $Ba_{0.82}K_{0.18}Fe_2As_2$ almost show no in-plane resistivity anisotropy and meanwhile the normal state resistivity does not follow the T-linear behavior. The correspondence between the anisotropy and T-linear behavior of resistivity presents in all of measured materials. We did not find a single exception.

Our above results have important implications for the origin of the nematicity in iron-pnictides. First, our results strongly support the nematic state in iron-pnictides is indeed an electronic nematic state. Our measurements show that the in-plane resistivity anisotropy is closely related to the magnetic transition rather than the structural transition and persists at temperature higher than structural transition, suggesting the existence of nematicity even in tetragonal lattice structure. Second, the distinct anisotropy of resistivity between the hole and electron underdoped materials reveals the hidden interplay between magnetic and orbital degrees of free-

dom. Recently, many theories focus on orbital ordering which generates an unequal occupation of d_{xz} and d_{yz} orbitals[28] that breaks the rotational symmetry and causes the lattice distortion[29]. ARPES measurements have provided orbital ordering evidence[15]. Since there is little anisotropy in the hole doped samples in their magnetically ordered states, our results suggest that the resistivity anisotropy is most likely induced by orbital ordering rather than magnetic ordering. The orbital ordering is suppressed rapidly by hole-doping while it is relatively robust to electron-doping. The strong enhancement of the anisotropy around T_N in electron doped systems indicates that the magnetic ordering and orbital ordering are intimately connected to each other in these systems. However, our result on hole doped samples suggest the magnetic ordering is not simply a result of orbital ordering. Considering the facts that the dominating orbitals are t_{2g} and the orbital ordering is most likely due to the d_{xz} and d_{yz} , we can conclude that although the magnetically ordered states in both electron and hole doped materials have an identical ordering wavevector, the two states must differ microscopically from their orbital involvements, namely, the magnetism is orbital selective in a way that the magnetic ordering in hole-doped systems is attributed mostly from the d_{xy} orbital while the d_{yz} and d_{xz} make important contributions to the magnetism in the electron doped ones. This implication can be tested explicitly by ARPES experiments in hole doped materials. Finally, the correspondence between the anisotropy and T-linear behavior suggests the importance of electron-electron correlation in causing the orbital and magnetic ordering. The non-Fermi liquid behavior of T-linear resistivity can be understood by the presence of strong orbital or magnetic fluctuations in all three t_{2g} orbitals. Consequently, the suppression of the non-fermi liquid behavior by hole-doping indicates the suppression of orbital and magnetic fluctuations in the d_{xz} and d_{yz} ones.

In conclusion, we have measured the in-plane resistivity anisotropy on electron-underdoped $\text{EuFe}_{2-x}\text{Co}_x\text{As}_2$ and $\text{BaFe}_{2-x}\text{Co}_x\text{As}_2$, and hole-underdoped $\text{Ba}_{1-x}\text{K}_x\text{Fe}_2\text{As}_2$ single crystals. Large in-plane resistivity anisotropy was found in $\text{EuFe}_{2-x}\text{Co}_x\text{As}_2$ which is quite similar to the isostructural $\text{BaFe}_{2-x}\text{Co}_x\text{As}_2$ system, however anisotropy disappears in hole-doped samples. We identified an universal correspondence between the anisotropy and a T-linear behavior of resistivity at high temperature. The different behavior of the anisotropy at T_N and T_S rules out the anisotropy is originated from the lattice degree of freedom. The magnetic states in the hole and electron doped systems are significantly different.

This work is supported by the Nature Science Foundation of China, Ministry of Science and Technology and by Chinese Academy of Sciences.

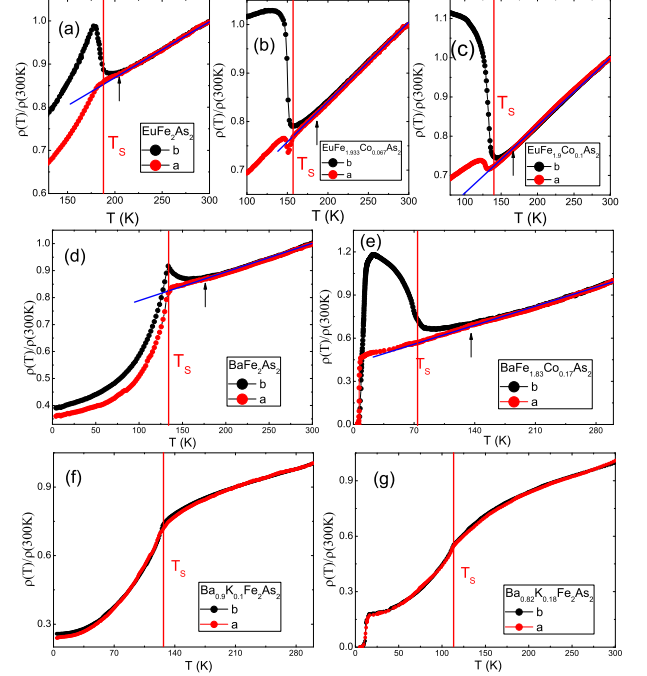


FIG. 4: (Color online) The temperature dependence of ρ_a and ρ_b for (a) EuFe_2As_2 , (b): $\text{EuFe}_{1.933}\text{Co}_{0.067}\text{As}_2$, (c): $\text{EuFe}_{1.9}\text{Co}_{0.1}\text{As}_2$, (d): BaFe_2As_2 , (e): $\text{BaFe}_{1.83}\text{Co}_{0.17}\text{As}_2$, (f): $\text{Ba}_{0.9}\text{K}_{0.1}\text{Fe}_2\text{As}_2$ and (g): $\text{Ba}_{0.82}\text{K}_{0.18}\text{Fe}_2\text{As}_2$. The black arrows indicate the temperature where ρ_a and ρ_b begin to show discrepancy. The red line indicates the T_S . The blue line is the linear fit of the resistivity above the black arrow indicated temperature.

- [1] Y. Kamihara *et al.*, *J. Am. Chem. Soc.* **130**, 3296(2008).
- [2] X. H. Chen *et al.*, *Nature* **453**, 761(2008).
- [3] Z. A. Ren *et al.*, *Europhys. Lett.* **83**, 17002(2008).
- [4] M. Rotter *et al.*, *Phys. Rev. Lett.* **101**, 107006(2008).
- [5] F. Krger *et al.*, *Phys. Rev. B* **79**, 054504 (2009).
- [6] C. Fang *et al.*, *Phys. Rev. B* **77**, 224509 (2008).
- [7] C. Xu *et al.*, *Phys. Rev. B* **78**, 020501 (2008).
- [8] Jiun-Haw Chu *et al.*, *Science* **329**, 824 (2010).
- [9] M. A. Tanatar *et al.*, *Phys. Rev. B* **81**, 184508 (2010).
- [10] Y. Ando *et al.*, *Phys. Rev. Lett.* **88**, 137005 (2002).
- [11] V. Hinkov *et al.*, *Science* **319**, 597 (2008).
- [12] M. P. Lilly *et al.*, *Phys. Rev. Lett.* **82**, 394 (1999).
- [13] R. A. Borzi *et al.*, *Science* **315**, 214 (2007).
- [14] Jun Zhao *et al.*, *Nature Physics* **5**, 555 (2009).
- [15] T. Shimojima *et al.*, *Phys. Rev. Lett.* **104**, 057002 (2010).
- [16] T.-M. Chuang *et al.*, *Science* **327**, 181 (2010).
- [17] Chi-Cheng Lee *et al.*, *Phys. Rev. Lett.* **103**, 267001 (2009).
- [18] B. Valenzuela *et al.*, *Phys. Rev. Lett.* **105**, 207202(2010).
- [19] X. F. Wang *et al.*, *Phys. Rev. Lett.* **102**, 117005(2009).
- [20] T. Wu *et al.*, *J. Magn. Magn. Mater.* **321**, 3870 (2009).
- [21] Y. He *et al.*, *J. Phys.: Condens. Matter* **22**, 235701

- (2010).
- [22] J. J. Ying *et al.*, Phys. Rev. B **81**, 052503 (2010).
- [23] Zhi Ren *et al.*, Phys. Rev. B **78**, 052501 (2008).
- [24] G. Wu *et al.*, J. Phys.: Condens. Matter **20**, 422201 (2008).
- [25] Jiun-Haw Chu *et al.*, Phys. Rev. B **79**, 014506 (2009).
- [26] S. Kasahara *et al.*, Phys. Rev. B **81**, 184519 (2010).
- [27] R. H. Liu *et al.*, Phys. Rev. Lett **101**, 087001 (2008).
- [28] C.-C. Chen *et al.*, Phys. Rev. B **82**, 100504(R) (2010).
- [29] Weicheng Lv *et al.*, Phys. Rev. B **82**, 045125 (2010)